Study of hygroscopic behaviour of spruce during adsorption and desorption

X Zhou[1], G Desmarais[2], D Mannes[3], D Derome[4] and J Carmeliet[1]

[1] Chair of Building Physics, ETH Zürich, Zürich, Switzerland
[2] Planair SA, Building Physics and Building Retrofit Groups, Geneva, Switzerland
[3] Laboratory for Neutron Scattering and Imaging, Paul Scherrer Institute, Villigen, Switzerland
[4] Department of Civil and Building Engineering, Université de Sherbrooke, Sherbrooke, Canada

xizhou@ethz.ch

Abstract. Sorption of water vapour in hygroscopic porous materials is associated with latent heat release and absorption. This phenomenon should be taken into account to achieve a better understanding of the coupled transfer of vapour and heat in hygroscopic porous materials. In this paper, water vapour adsorption and desorption in the longitudinal direction of spruce samples are studied. Neutron radiography is used to measure changes in moisture content and wireless thermocouples are used to measure temperature changes. During the adsorption and desorption experiments, large changes in moisture content and temperature are observed. A hygrothermal model is developed to simulate vapour and heat transfer during adsorption and desorption experiments. Generally, the numerical model predicts well the measured moisture and temperature changes. The large moisture change is due to the low vapour resistance factor in the longitudinal direction of the spruce samples. The latent heat associated with vapour adsorption is the cause of the large temperature changes. It was found that vapour permeability affects both vapour and heat transfer, while thermal conductivity only affects heat transfer.

1. Introduction

The capability of hygroscopic materials to moderate indoor humidity changes has been extensively studied [1,2]. Moisture buffering effect in wall envelopes could reduce indoor humidity fluctuations and thus can reduce the risk of moisture-related damage. The latent heat release/absorption associated with moisture adsorption/desorption in hygroscopic materials could impact indoor thermal comfort and building energy consumption. Hygroscopic materials can undergo significant changes in temperature as a result of moisture adsorption or desorption.

Wood is an organic, hygroscopic and natural hierarchical material. Due to its hygrothermal, acoustic, mechanical, and aesthetic properties, it is very suitable to be used as a building material. Compared to other building materials, wood is sustainable, easy to recycle and environmentally friendly. Buildings designed with engineered timber can reach more than 80 m in height nowadays. Wood has much smaller embodied carbon emissions compared to concrete and steel. Furthermore, wood can turn buildings into

a carbon sink where CO_2 from air is turned into glucose and then wood polymers [3]. The use of wooden materials provides solid measures to reduce carbon emissions and mitigate climate change.

Coupled moisture and heat transport during adsorption and desorption is often studied in terms of total mass change. Moisture change at spatial scales is often lacking. Therefore, this work uses state-of-the-art experiments and numerical models to study moisture and temperature transport in wood during adsorption and desorption. Both temporal and spatial changes of moisture content and temperature are documented and analyzed. The effect of important parameters on moisture and heat transport is then discussed.

2. Experimental methodology

Norway spruce samples, with a size of 85 mm (radial) x 32.7 mm (longitudinal) x 10.0 mm (tangential), are used here for the adsorption and desorption experiments (Figure. 1a). The wood samples are cut from a source of Norway spruce characterized by Zillig [4]. The dry bulk density of the samples is 318.1 kg/m^3. Samples are equilibrated as follows: the sample for the adsorption experiment is stored in a desiccating cabinet with silica gel particles and the sample for the desorption experiment is stored in a cabinet over $NH_4H_2PO_4$ solution. The initial moisture content of the samples for the adsorption and desorption experiment is 0.019 and 0.175 kg/kg, respectively, which corresponds to a relative humidity of 5.5% RH and 90.5%RH, according to the DVS-obtained sorption curves in Figure 6.

The sample is fixed inside a tailor-made micro-wind tunnel. The walls of the tunnel are made of extruded polystyrene insulation (EPX) to minimize lateral heat and moisture exchanges. Only the top surface of the sample is exposed to the air flow. The test consists of two periods: the conditioning period and the experimental period. In the conditioning period, the sample is subjected to air flow at a controlled speed of 1.5 m/s and a controlled temperature of 30.0 °C. For the adsorption sample, the relative humidity of the incoming air is around 3%, which is similar to the initial humidity of the sample. For the desorption sample, the relative humidity of the incoming air is 82.5% RH, which is a little lower than the initial relative humidity of the sample. As a result, there is a decrease in moisture in the desorption sample in the conditioning period. The conditioning period is terminated when the weight and temperatures in the samples become stable. In the experimental period, the air flow is also maintained at the speed of 1.5 m/s and temperature of 30.0 °C. For the adsorption sample, the relative humidity of the air is increased rapidly from 3% RH to around 82.5% RH. For the desorption sample, the relative humidity of the air is decreased rapidly from 82.5% RH to around 3% RH.

High-gage wireless thermocouples are used to measure temperature change during the experiments. The wireless thermocouples are chosen to avoid the interference of wires so that the total weight variation throughout the experiment could be accurately measured. The thermocouples are located 3.0, 6.2, 10.6, 15.9, 22.6 and 30.0 mm from the top surface (Figure. 1b), and inserted in horizontal tiny holes. The total moisture content variation is acquired with balances. The spatial change of moisture content is recorded with neutron radiography. Neutron radiography quantification is based on intensity measurements of a neutron beam transmitted through an object. It has been used to measure the time- and space-resolved moisture content distribution in wood and other porous building materials [5–8]. The experiments were carried out at the neutron imaging beamline ICON at the Paul Scherrer Institute in Villigen, Switzerland [9]. The Quantitative Neutron Imaging (QNI) algorithm [6], which is based on the iterative reconstruction of the measured image by overlapping point scattered functions calculated using Monte-Carlo simulation, is used to obtain the moisture content change. As wood swells (shrinks) during adsorption (desorption), an affine registration process is applied to the images obtained following the initial corrections. Here the moisture content change at the locations of the thermocouples is presented. The accuracy of temperature measurement is 0.1 °C. Based on the study of [10], the estimated accuracy of moisture content measurement by neutron radiography is 1.0%.

Figure 2 presents the change of total moisture in the wood samples measured by balance and Neutron radiography. The measured result by Neutron radiography is very close to that by balance. The total moisture change in the desorption experiment is larger than in the adsorption experiment. The temperature and moisture content change at the left and right thermocouples are very similar to each

other. We present here the results taken at the left side of the sample. Figures 3 and 4 present the moisture content variation at the location of thermocouples for the adsorption and desorption experiments. Moisture content change is larger close to the top surface than at deeper depth. The rate of moisture change is larger at the beginning of the experiments and it decreases gradually with time. Compared to the adsorption experiment, there is more moisture change during the desorption experiment. Figures 5 and 6 present the temperature variation at the location of thermocouples for the adsorption and desorption experiments. During the adsorption and desorption experiment, there is a very large change of temperature at the very beginning of the experiment. Then the temperature change becomes smaller gradually. The temperature change is larger in the adsorption experiment than in the desorption experiment. For example, the largest temperature change is 7.8 °C at location 1 during the adsorption experiment while it is only 5.2 °C at this location during the desorption experiment.

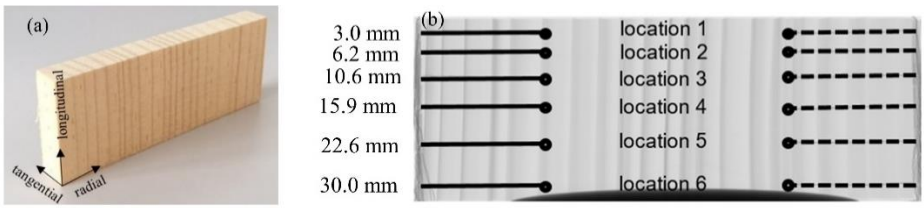

Figure 1. (a) Illustration of a spruce sample; (b) Location of thermocouples in the spruce sample

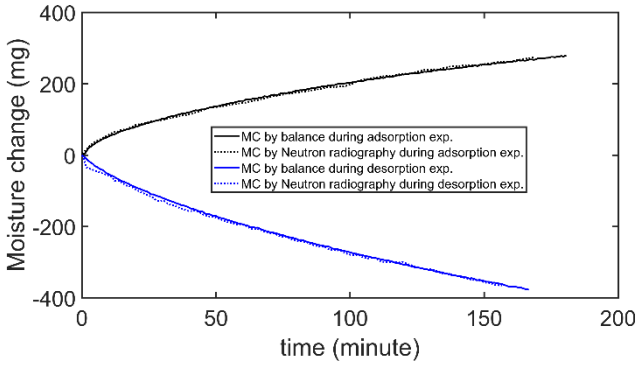

Figure 2. Moisture change in the adsorption and desorption experiment (MC: moisture change)

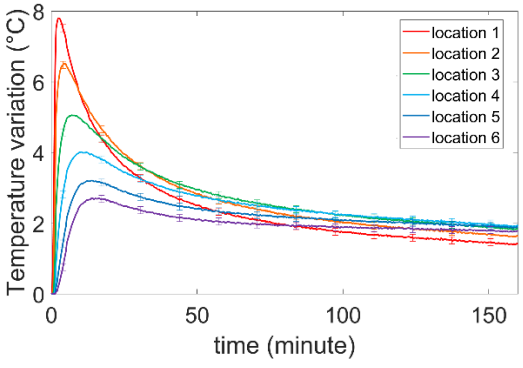

Figure 3. Moisture content (MC) variation during adsorption experiment

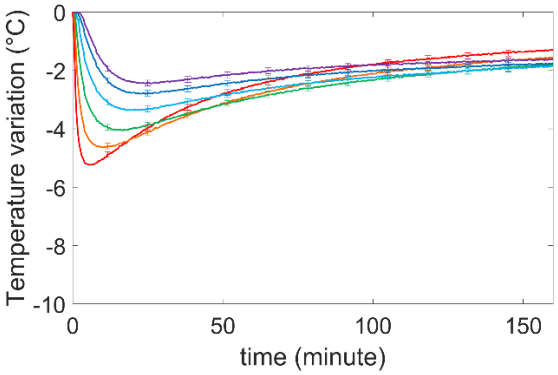

Figure 4. Moisture content (MC) variation during desorption experiment

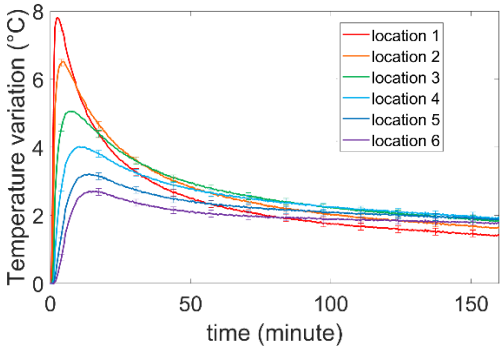

Figure 5. Temperature variation during adsorption experiment.

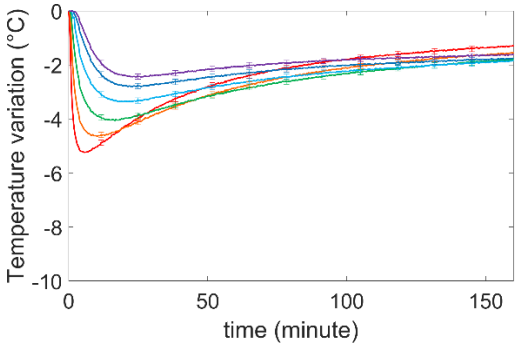

Figure 6. Temperature variation during desorption experiment.

3. Numerical simulations

The governing equations for three-dimensional coupled moisture and heat transport in the wood sample are based on [11,12]. The main relationships are presented here. Wood is an orthotropic material and therefore material properties in the longitudinal, tangential, and radial directions are different. Vapour transport in the wood is described with Fick's Law. The governing equation of moisture conservation is:

$$\frac{\partial w}{\partial p_c}\frac{\partial p_c}{\partial t}+\frac{\partial}{\partial x_i}g_v=0 \tag{1}$$

with vapour flow:

$$g_v=-\delta_{i,j}(w)\cdot\frac{p_v}{\rho_l\cdot R_v\cdot T}\cdot\frac{\partial p_c}{\partial x_j}-\delta_{i,j}(w)\cdot\frac{p_v}{\rho_l\cdot R_v\cdot T^2}(\rho_l\cdot L_v)\cdot\frac{\partial T}{\partial x_j} \tag{2}$$

The governing equation of energy conservation is:

$$(c_0\cdot\rho_0+c_l\cdot w)\cdot\frac{\partial T}{\partial t}+\nabla\cdot((c_v\cdot(\mathrm{T}-\mathrm{T}_{ref})+L_m)\cdot g_v)=-\frac{\partial}{\partial x_i}(\lambda_{i,j}(w)\frac{\partial T}{\partial x_j}) \tag{3}$$

where w is the moisture content (kg/m^3), p_c is the capillary pressure (Pa), g_v is the vapour flow flux (kg/m^{2}s), i, j=1, 2, 3 (x_1=x, x_2=y, x_3=z), $\delta_{i,j}$(w) is the water vapour permeability (s), p_v is the vapour pressure (Pa), ρ_l is the density of sorbed water (kg/m^3), R_v is the gas constant of water (J/kg K), T is the temperature (K), c_0 is the specific heat capacity of spruce (J/kg K), c_l is the specific heat capacity of water (J/kg K), c_v is the specific heat capacity of vapour (J/kg K), ρ_0 is the density of spruce (kg/m^3), T_{ref} is the reference temperature (273.15 K), L_m is the latent heat of moisture in wood (J/kg), $\lambda_{i,j}$(w) is the thermal conductivity (W/mK). We note that $\delta_{i,j}$(w) and $\lambda_{i,j}$(w) are function of water content.

The adsorption and desorption isotherms are described with the Guggenheim-Anderson-de Boer (GAB) model [13]:

$$w=\frac{w_m ck\phi}{(1-k\phi)(1+k(c-1)\phi)} \tag{4}$$

where w is the equilibrium moisture content (kg/kg), Φ is the relative humidity, w_m, c and k are the fitting parameters. The hygroscopic sorption is measured with DVS Endeavour that has a mass resolution of 1 µg. The sorption isotherms are determined at 30.0 °C. The equilibrium criterion (dm/dt) for the DVS instrument is 0.002%/min for a minimum of 60 minutes. For the adsorption experiment, the sample follows the main adsorption curve. For the main adsorption curve, the sample is first dried to 0 % RH, followed by progressive sampling from 10 to 90 % RH in 10 % RH increments, followed by sampling at 95 % RH. The main desorption curve is measured by reversing the humidity steps. The desorption experiment follows a desorption scanning curve. Therefore, a desorption scanning curve is measured. The sample is first adsorbed to 90 % RH, then followed by sampling from 90% to 30% RH in 10% RH increments. Figure 7 shows the sorption curves of the samples.

The vapour resistance factor of the spruce is described with an exponential function:

$$\mu = \frac{1}{a + b \cdot \exp(c \cdot RH)} \tag{5}$$

where *a*, *b* and *c* are model parameters. Vapour transport is predominately in longitudinal direction, thus vertically for this experimental setup. The vapour resistance in radial and tangential directions has negligible influence on the longitudinal vapour transport. Vapour resistance factor in these two directions is obtained from Zillig [4]. For the longitudinal direction, the values of a, b and c are obtained by comparing simulated and measured moisture results. The relation between vapour permeability and vapour resistance factor is:

$$\delta_v = \frac{\delta_a}{\mu} \tag{6}$$

where δ_a is the vapour permeability in dry air , which is given by the Schirmer's equation. Figure 8 shows the vapour resistance factor in the three directions of spruce. The vapour resistance factor in the longitudinal direction is much smaller than in the radical and tangential direction. The low vapour resistance factor in the longitudinal direction leads to fast vapour transport in the samples.

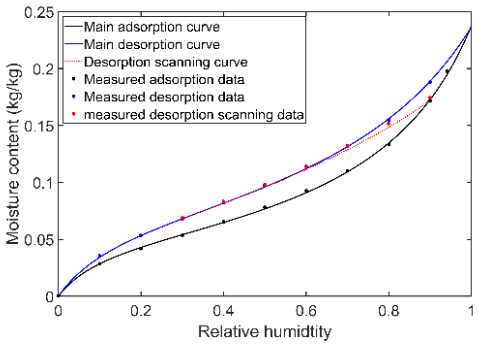

Figure 7. Sorption curves of the spruce

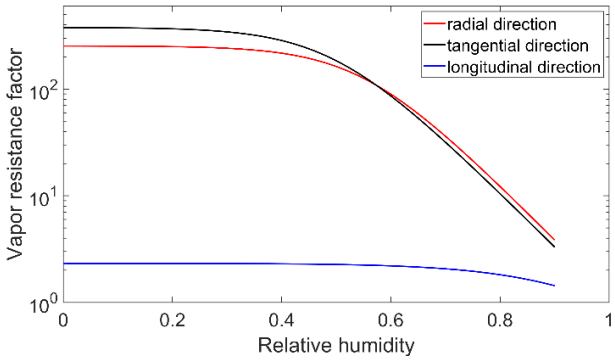

Figure 8. Vapour resistance factor in the different directions of spruce sample

The enthalpy of sorbed water is smaller than that of liquid water. When the adsorbed water in the wood evaporates, the associated latent heat is the sum of latent heat of vapourization of water and the differential heat of sorption. The differential heat of sorption in wood can be calculated based on two isotherms at different temperatures and calculated using the Clausius-Clapeyron equation:

$$h_s = R_v \frac{\ln RH_2 - \ln RH_1}{\frac{1}{T_1} - \frac{1}{T_2}} \tag{7}$$

The adsorption and desorption isotherms at 20 and 40 °C are used for the calculation of the differential heat of sorption. Figures 9 and 10 shows the differential heat of sorption for adsorption and desorption experiments.

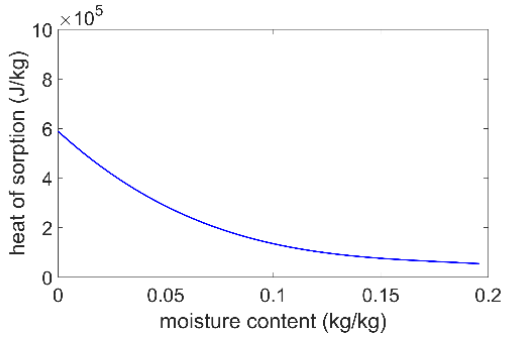

Figure 9. Differential heat of sorption for the adsorption experiment

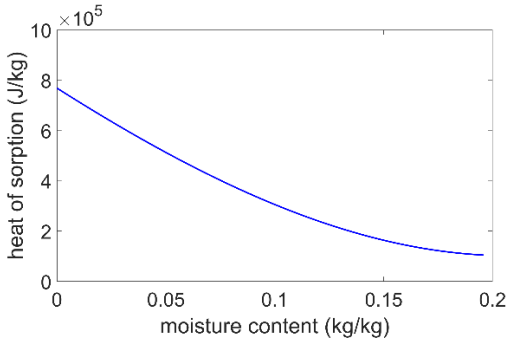

Figure 10. Differential heat of sorption for the desorption experiment

4. Result

The simulated and measured temperature and moisture content changes in the adsorption experiment and desorption experiments are compared in Figures 11 and 12. Generally speaking, the experimental results are very close with the simulated ones. The numerical model simulates well the large temperature change at the beginning of both experiments. The large temperature change at the beginning of the adsorption and desorption experiment is due to the large adsorption and desorption rate. The large moisture change rate is associated with the large release and absorb of latent heat. The difference between measured and simulated results could be caused by material heterogeneity. The latent heat of vapourization is 2.437×10^6 J/kg. Therefore, the differential heat of sorption is much smaller than the latent heat of vapourization. Therefore, the effect of the differential heat of sorption on temperature change is much smaller than that of latent heat of vapourization.

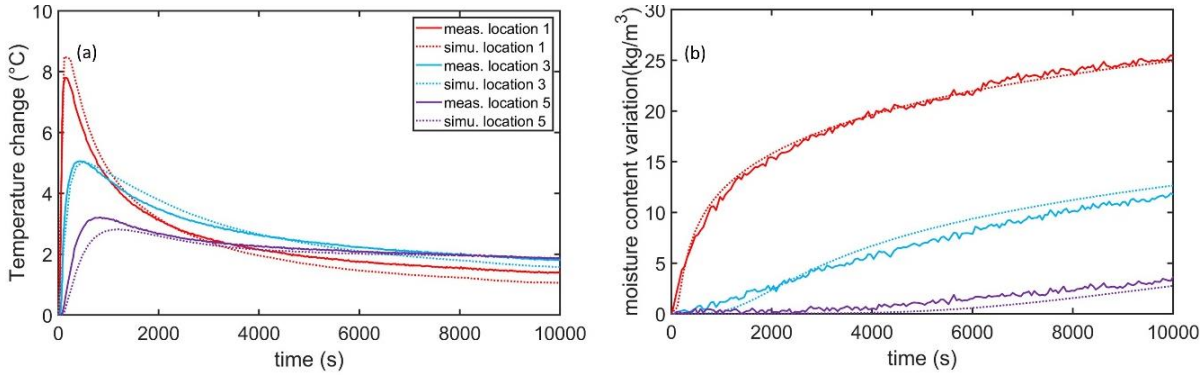

Figure 11. Comparison of measured and simulated temperature and moisture content change in the adsorption experiment

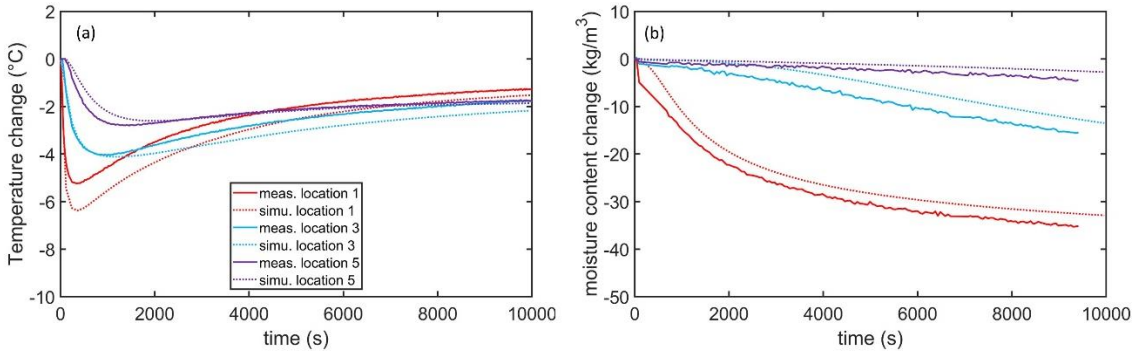

Figure 12. Comparison of measured and simulated moisture and temperature change in the desorption experiment

Vapour resistance factor and thermal conductivity are the most important parameters influencing vapour and heat transport. The effect of these two parameters is evaluated by varying their values. Figure 13 shows the effect of thermal conductivity on moisture content and temperature changes. Thermal conductivity hardly affects changes in moisture content, whereas it has a very large effect on temperature changes. The heat transport will be faster with a larger thermal conductivity. In contrast, the moisture content and temperature changes are significantly affected by the vapour resistance factor (Figure 14). The vapour transport will be faster with a smaller vapour resistance factor, leading to larger moisture content change. At the same time, a larger change in moisture content involves more latent heat released during the adsorption process. As a result, the temperature increase will be larger due to a decrease in the vapour resistance coefficient. Therefore, the vapour resistance factor affects both moisture and heat transfer, while thermal conductivity only affects heat transfer.

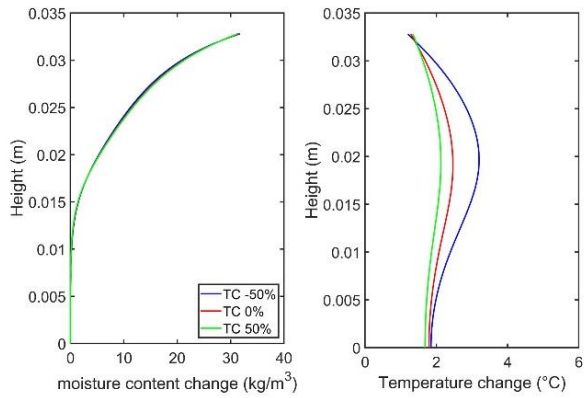

Figure 13. Influence of thermal conductivity (TC) on moisture content and temperature change at t=4800s during the adsorption.

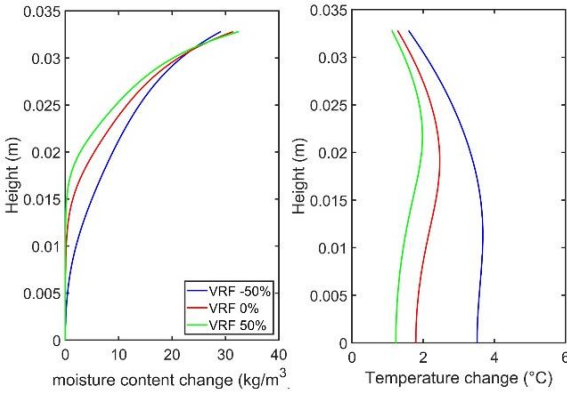

Figure 14. Influence of vapour resistance factor (VRF) on moisture content and temperature change at t=4800s during the adsorption.

5. Conclusions

Vapour adsorption and desorption experiments are performed to study vapour and heat transfer in spruce samples. During the experiment, neutron radiography and wireless thermocouples are used to measure moisture content and temperature changes. Large changes in moisture content and temperature are observed at the onset of both adsorption and desorption experiments. A hygrothermal model is used to simulate the vapour and heat transfer during the adsorption and desorption experiments. Generally, the

numerical model predicts well the measured moisture and temperature changes. The large moisture sorption rate results in large temperature changes during the adsorption and desorption process, which is due to the low vapour resistance factor in the longitudinal direction of the spruce. It has been found that the vapour resistance coefficient affects both vapour and heat transfer, while thermal conductivity only affects heat transfer.

Acknowledgments
Stephan Carl and Bruno Binder are greatly appreciated for their help with the experiments.

References

[1] Osanyintola O F, Talukdar P and Simonson C J 2006 Effect of initial conditions, boundary conditions and thickness on the moisture buffering capacity of spruce plywood *Energy Build.* **38** 1283–92
[2] Carmeliet J, Blocken B, Defraeye T and Derome D 2011 10 Moisture phenomena in whole building performance prediction *Build. Perform. Simul. Des. Oper.* 277
[3] Churkina G, Organschi A, Reyer C P O, Ruff A, Vinke K, Liu Z, Reck B K, Graedel T E and Schellnhuber H J 2020 Buildings as a global carbon sink *Nat. Sustain.* 1–8
[4] Zillig W 2009 Moisture transport in wood using a multiscale approach *Kathol. Univ. Leuven, Leuven, Belgium*
[5] Zhou X, Desmarais G, Vontobel P, Carmeliet J and Derome D 2020 Masonry brick–cement mortar interface resistance to water transport determined with neutron radiography and numerical modeling *J. Build. Phys.* 1744259120908967
[6] Hassanein R, Meyer H O, Carminati A, Estermann M, Lehmann E and Vontobel P 2006 Investigation of water imbibition in porous stone by thermal neutron radiography *J. Phys. D. Appl. Phys.* **39** 4284–91
[7] Sonderegger W, Mannes D, Kaestner A, Hovind J and Lehmann E 2015 On-line monitoring of hygroscopicity and dimensional changes of wood during thermal modification by means of neutron imaging methods *Holzforschung* **69** 87–95
[8] Lämmlein S L, Mannes D, Van Damme B, Schwarze F W M R and Burgert I 2019 The influence of multi-layered varnishes on moisture protection and vibrational properties of violin wood *Sci. Rep.* **9** 1–9
[9] Kaestner A P, Hartmann S, Kühne G, Frei G, Grünzweig C, Josic L, Schmid F and Lehmann E H 2011 The ICON beamline–A facility for cold neutron imaging at SINQ *Nucl. Instruments Methods Phys. Res. Sect. A Accel. Spectrometers, Detect. Assoc. Equip.* **659** 387–93
[10] Boillat P, Carminati C, Schmid F, Grünzweig C, Hovind J, Kaestner A, Mannes D, Morgano M, Siegwart M and Trtik P 2018 Chasing quantitative biases in neutron imaging with scintillator-camera detectors: a practical method with black body grids *Opt. Express* **26** 15769–84
[11] Janssen H, Blocken B and Carmeliet J 2007 Conservative modelling of the moisture and heat transfer in building components under atmospheric excitation *Int. J. Heat Mass Transf.* **50** 1128–40
[12] Zhou X, Carmeliet J and Derome D 2020 Assessment of moisture risk of wooden beam embedded in internally insulated masonry walls with 2D and 3D models *Build. Environ.* 107460
[13] Guggenheim E A 1966 Applications of statistical mechanics